Title: Development of an RT-RPA assay for La Crosse virus detection provides insights into age-dependent neuroinvasion in mice

Authors: Lily Lumkong[1], Reem Alatrash[1], Sainetra Sridhar[1], Bobby Brooke Herrera[1,2]

Affiliations:

[1]Rutgers Global Health Institute, Rutgers University, New Brunswick, NJ, USA

[2]Department of Medicine, Division of Allergy, Immunology, and Infectious Diseases, and Child Health Institute of New Jersey, Rutgers Robert Wood Johnson Medical School, Rutgers University, New Brunswick, NJ, USA

***Corresponding Author**: BBH, bherrera@globalhealth.rutgers.edu

Keywords: La Crosse virus, Reverse transcription recombinase polymerase amplification, Lateral flow assay, Neuroinvasion, Age-susceptible mouse model

Abstract

La Crosse virus (LACV) is a mosquito-borne arbovirus that causes pediatric encephalitis in North America, primarily affecting children under the age of 16 years of age. Early and accurate diagnosis is crucial to reducing morbidity in this vulnerable population; however, existing molecular and serological methods face limitations in sensitivity, specificity, and accessibility. Here, we present the development of a reverse transcription recombinase polymerase amplification (RT-RPA) assay for LACV detection. Our assay detects LACV within 20 minutes with a limit of detection of 100-1000 viral copies, demonstrating high specificity without cross-reactivity against closely related or geographically relevant arboviruses. We further integrate the RT-RPA assay into a lateral flow format, potentially enabling simple and inexpensive point-of-care diagnosis. To complement our assay development, we investigated viral pathogenesis in a mouse model that recapitulates the age-dependent susceptibility observed in human populations. Using this RT-RPA assay, we reveal that LACV invades the brains of weanling mice as early as 4 days post-infection (dpi) and adult mice by 5 dpi. Surviving adult mice had no detectable virus within their brains by 20 dpi. These results underscore the utility of our RT-RPA-based platform for LACV diagnosis and offer novel insights into the age-dependent temporal dynamics of LACV neuroinvasion and viral clearance.

Introduction

La Crosse virus (LACV) is a single-stranded, negative-sense virus within the *Peribunyaviridae* family, order *Bunyavirales*, and is classified under the California serogroup (CSG) viruses [1, 2]. Members of this viral family possess a distinctive tri-segmented genome composing the small (S), medium (M), and large (L) segments. The S segment of LACV encodes both the nucleocapsid (N) protein and a nonstructural protein (NSs) implicated in the disruption of host innate immune responses [3, 4]. The M segment encodes glycoproteins Gn and Gc, which mediate viral attachment and entry, alongside a nonstructural protein (NSm) crucial for virion assembly [5]. The L segment encodes the RNA-dependent RNA polymerase (RdRp), an enzyme integral to viral genome transcription and replication [6-8].

LACV was first identified in La Crosse, Wisconsin in the 1960s, and has since remained endemic in North America, particularly in the Midwestern and Eastern United States, including the Appalachian corridor [9]. Its principal vector is the Eastern treehole mosquito, *Aedes triseriatus*, although more recent data indicate that *Aedes albopictus* and *Aedes japonicus* may also contribute to transmission, raising concerns about geographic expansion [10-12]. Between 2020 and 2023, the Centers for Disease Control and Prevention (CDC) documented 182 LACV-related hospitalizations in the United States – most of which affected pediatric patients – yet the actual incidence is likely underestimated due to underreporting and diagnostic limitations [7, 13, 14]. Furthermore, snowshoe hare virus (SSHV) – a closely related CSG virus that shares approximately 89% sequence identity with LACV – circulates endemically in Canada and has also been associated with outbreaks in young populations, highlighting that

arboviruses within the CSG pose a broad threat to populations across North America [15, 16].

Human infections with LACV exhibit a wide spectrum of outcomes. While most cases remain asymptomatic or present as mild febrile illness, a subset of infections progress to severe central nervous system (CNS) involvement, resulting in encephalitis, seizures, altered mental status, and, in rare instances, coma or fatality [17]. Children under 16 years of age are particularly susceptible to adverse outcomes, a pattern attributed in part to differences in immune responses and blood brain barrier function [10, 18-23].

Despite its clinical importance, LACV remains difficult to diagnose. Conventional methods such as reverse transcription quantitative polymerase chain reaction (RT-qPCR) provide high sensitivity and specificity during peak viremia, yet its utility diminishes once viral titers wane [13, 24-27]. Serological tools, including enzyme-linked immunosorbent assays (ELISAs), can identify LACV-specific antibodies, but often require confirmatory plaque reduction neutralization tests (PRNTs) to differentiate infections from LACV and closely related viruses [28]. Moreover, the absence of commercially available LACV-specific RT-qPCRs and ELISAs, and the labor-intensive nature of PRNTs, limit the scalability of these approaches, especially in areas with restricted diagnostic resources.

To address these diagnostic hurdles, recombinase polymerase amplification (RPA) has emerged as a promising isothermal nucleic acid amplification technology [29]. By functioning at 37-42°C and completing amplification in as few as 20 minutes, RPA reduces the need for specialized equipment. This method employs recombinase

enzymes to bind primers to homologous sequences, single-stranded DNA-binding proteins to stabilize the resulting complexes, and strand-displacing polymerases to drive rapid amplification [30-32]. When combined with reverse transcription (RT-RPA), the method allows rapid detection of RNA viruses like LACV through an initial conversion of RNA into cDNA. Furthermore, RPA amplicons can be evaluated using standard gel electrophoresis or via lateral flow assays (LFAs), the latter providing near-instantaneous visual results suitable for field-based or point-of-care settings [27, 33]. LFAs capitalize on capillary action within a nitrocellulose strip, where labeled detection reagents bind to specific target amplicons, generating visible test and control lines [34-36].

In addition to the critical need for improved diagnostics, LACV exhibits age-dependent pathogenicity that requires further investigation. Notably, the age-dependent disease severity observed in humans is recapitulated in murine models, where weanling (3 week old) mice display higher mortality rates and more pronounced CNS pathology compared to adult (≥6 week old) mice [7, 9, 21, 37, 38]. While the pathogenesis of LACV has been relatively well studied in mice and other mammals, limited data are available regarding the temporal dynamics of LACV neuroinvasion into the CNS and/or brain [15, 39, 40].

In this study, we describe the development and validation of an RT-RPA assay to detect LACV with high sensitivity and specificity. We also utilize an age-susceptible mouse model to characterize the temporal progression of LACV infection in the brain, exploring how host age influences both neuroinvasion and viral clearance. Our study seeks to enhance early detection in endemic regions and improve the broader understanding of host-pathogen interactions in LACV encephalitis.

Results

Screening of RT-RPA primer pairs for LACV detection

To identify a genome segment best suited for specific and sensitive detection of LACV, we performed a percentage identity matrix analysis on the S, M, and L segments from a panel of CSG viruses. These included LACV, SSHV, Khatanga virus, California Encephalitis virus, San Angelo virus, Lumbo virus, and Tahnya virus, and one virus from the Melaka virus family, Jamestown Canyon virus. Based on homology analyses of DNA sequences, the S, M, and L segments displayed homology ranging from 76.1-88%, 69-78.8%, and 73.7-81.6%, respectively (Fig. 1, Table 1). Since the M segment exhibited the greatest divergence between LACV and other CSG viruses, we selected it as the target for LACV-specific primer design.

Four primer pairs were generated, each producing amplicons of at least 100 base pairs. These primers were tested at 37°C, 39°C, and 42°C for 20 minutes. Primer pair 3 at 39°C yielded the clearest and most intense amplification band (208 base pairs [bp]) and was chosen for subsequent optimization (Fig. 2). Primer pair 4 also showed reliable results (240 bp), but was slightly less optimal.

Assessing LACV RT-RPA amplification time and analytical sensitivity and specificity via gel electrophoresis

After identifying the best performing primer pair, we conducted a time course study to determine the minimal incubation period necessary for effective RT-RPA detection of LACV. Reactions were incubated for 5, 10, 20, and 60 minutes before the

amplicons were visualized by agarose gel electrophoresis. Although faint bands appeared as early as 10 minutes, we observed optimal band clarity and intensity at 20 minutes (Fig. 3A).

Next, we evaluated the RT-RPA assay's analytical sensitivity using a ten-fold serial dilution of LACV RNA, ranging from 10^5 to 0 input copies in the RT step. The limit of detection (LOD) was established at 100-1000 copies (Fig. 3B). To verify the RT-RPA assay's specificity, we tested RNA extracted from other arboviruses, including SSHV, dengue virus serotypes 1-4 (DENV-1-4), Zika virus (ZIKV), West Nile virus (WNV), and yellow fever virus (YFV). No amplification occurred in any non-LACV samples, confirming the specificity of our primer pair (Fig. 3C).

Integration of the LACV RT-RPA assay with an LFA

To enable the potential point-of-care diagnosis of LACV, a lateral flow assay (LFA) was developed and integrated with the LACV RT-RPA assay. We employed the same unlabeled forward primer, but the reverse primer was adapted to contain a 5'-biotin tag, combined with a short hybridization step in which the probe was labeled with a 5'-FAM tag. After RT-RPA and hybridization, the product was exposed to the LFA strip, containing detection lines coated with streptavidin on the test area and anti-rabbit antibody on the control area. Gold nanoparticle-conjugated anti-rabbit-FITC antibodies generated the visual signal upon binding to hybridization product containing the FAM and biotin labels. The LFA exhibited the same LOD of 100-1000 copies (Fig. 4A). Similarly, the LFA also did not cross-react with SSHV and the other geographically relevant arboviruses (Fig. 4B). These results confirm the LFA's utility as a potential rapid and field-deployable tool for LACV detection.

Evaluation of age-dependent detection and clearance of LACV in weanling and adult mouse brains

To probe how host age modulates LACV neuroinvasion, we utilized both weanling and adult C57BL/6 mice. Animals were inoculated intraperitoneally with 10^3 plaque forming units (PFU) of LACV, and brain tissues were collected at distinct days post-infection (dpi). Weanling mice were sampled at 2, 3, 4, 5, and 7 dpi, whereas adult mice were sampled at 4, 5, 6, 7, 10, and 20 dpi (Supplementary Fig. 1A). RNA from brain tissues was extracted, reverse transcribed to cDNA, and evaluated using RT-qPCR as well as the newly developed RT-RPA, and analyzed by both agarose gel electrophoresis and by LFA strips.

We observed that LACV reached the brains of weanling mice as early as 4 dpi, peaking at 5 dpi (Fig. 5A, Supplementary Fig. 1B). In adult mice, LACV was first detected at 5 dpi, with a plateau in detection between 6 and 10 dpi (Fig. 5B, Supplementary Fig. 1C). By 20 dpi, LACV was undetectable in the surviving adults, suggesting robust viral clearance. Variability was noted at 7 dpi in one weanling mouse and at 10 dpi in two adult mice, highlighting potential individual variation in viral replication and/or immune response and/or viral replication.

Discussion

In this study, we developed, optimized, and validated a novel RT-RPA assay to detect LACV. Traditional RT-qPCR techniques, although highly sensitive, rely on costly equipment and specialized laboratory settings, and often lose sensitivity as viral titers

decline [24, 25]. Serological tools, meanwhile, necessitate confirmatory plaque reduction neutralization tests (PRNTs) to differentiate among closely related arboviruses—a process that can be time-intensive and cumbersome for large-scale or field-based testing [26, 41]. Our RT-RPA assay addresses these limitations by demonstrating efficient and robust LACV detection with a LOD between 100 and 1000 copies and without cross-reaction. This performance was replicated in both agarose gel electrophoresis and LFA strips, underscoring the assay's versatility and potential utility in resource-constrained environments where on-site diagnostics could significantly improve patient management and epidemiological surveillance.

An important aspect of our assay's development was the primer design targeting the M segment. Using bioinformatic analysis of multiple CSG viruses, we observed greater sequence divergence in the M segment between LACV and closely related CSG viruses. By designing primers and probes that map specifically to these divergent regions, we achieved high specificity without any cross-reactivity against SSHV and other geographically relevant arboviruses [42]. These findings confirm that our assay is well suited to environments where multiple arboviruses circulate simultaneously. Moreover, the integrated approach of RT-RPA plus LFA reliably produced clear test lines, suggesting a potentially straightforward workflow for use in clinics or field settings lacking sophisticated equipment. In future iterations, combining the RT and RPA steps into a single reaction may further streamline testing by potentially eliminating the need for RNA extraction and cDNA synthesis.

Beyond diagnostic innovation, our data also elucidate important factors of LACV pathogenesis—particularly the impact of host age on the timing of neuroinvasion. We

employed a serial euthanasia approach to assess viral presence in the brains of weanling and adult mice at predefined intervals (2–7 dpi for weanlings; 4–20 dpi for adults). We demonstrated that weanling mice exhibited detectable virus in the brain as early as day 4 dpi, with viral loads peaking at days 5, and most weanling mice succumbing or displaying severe CNS pathology by the end of the study window. Conversely, in adult mice, LACV was first detected in the brain on day 5—indicating a delayed onset of neuroinvasion compared to weanlings—and attained peak levels around days 6–10. Notably, some adults still harbored detectable virus at 10 dpi, yet all surviving adults cleared the virus within the brain completely by 20 dpi. These findings suggest that adult mice experience a slower initial spread of virus into the CNS relative to weanlings, potentially allowing more time for immune responses to mitigate viral replication and promote survival. Although further immunological assays would be required to pinpoint the specific immune responses involved, the delayed neuroinvasion and ultimately effective viral clearance in adults likely underlie their more favorable clinical outcomes compared to younger hosts [21].

Taken together, our work underscores a dual contribution to the field: we introduce a highly sensitive and specific RT-RPA assay for LACV detection, and we leverage this assay to enhance our understanding of age-dependent neuroinvasion in a murine model. Importantly, the RT-RPA method is amenable to further refinements, such as one-step RT-RPA protocols or improved probe chemistries, which could streamline its use under outbreak conditions. From a public health perspective, quicker diagnoses in endemic or high-risk regions would facilitate timely interventions, especially for pediatric populations at greatest risk of severe outcomes. Meanwhile, our findings on

the timing and efficiency of viral invasion in adult versus weanling brains point toward an inherent advantage conferred by age-related immune maturity, reinforcing the notion that prophylactic or early therapeutic measures could be particularly impactful in children. Overall, these advancements promise to mitigate the burden of LACV disease and enrich our broader comprehension of arboviral neuroinvasion.

Methods

Multiple sequence alignments and primer/probe design

Percent identity matrix analysis was performed on the S, M, and L segments from a panel of CSG viruses. These included LACV (EF485031.1), SSHV (EU262553.1), Khatanga virus (KT288294.1), California Encephalitis virus (KX817313.1), San Angelo virus (KX817331.1), Lumbo virus (KX817325.1), Tahnya virus (EU622819.2), and Jamestown Canyon virus (HM007351.1). Multiple sequence alignments and homology analyses were generated using Clustal Omega (version 1.2.4). The resulting sequence alignments were subjected to phylogenetic analysis by constructing maximum-likelihood trees based on the Tamura-Nei model and 500 bootstrapping replications using Mega11 software.

Primers were manually designed using SnapGene software (version 8.0.1) (Supplementary Table 1), adhering to established RPA guidelines that limit the primer length to 30-35 bases, maintain 40-60% GC content, and minimize palindromic or repetitive sequences [32]. Primer candidates were initially tested in silico for hairpin and dimer formation. Those meeting these criteria underwent validation at three

temperatures, including 37°C, 39°C, and 42°C, for 20 minutes. The primer pair that yielded the strongest, most specific band was used in subsequent experiments.

RNA Extraction

The PureLink Viral RNA/DNA Mini kit (ThermoFisher) was used for RNA extraction from LACV (BEI Resources: NR-540), SSHV (BEI Resources: NR-535), DENV-1 (BEI Resources: Hawaii strain), DENV-2 (BEI Resources: DakArA1247 strain), DENV-3 (BEI Resources: CH53489 strain), DENV-4 (BEI Resources: H241 strain), ZIKV (BEI Resources: DAK AR 41524 strain), WNV (BEI Resources: Bird114 strain), and YFV (BEI Resources: YFV17D strain), following the manufacturer's instructions. Additionally, RNA from mouse brains was extracted using the RNeasy Lipid tissue Mini Kit (Qiagen), following the manufacturer's instructions. The concentration of the RNA extracts was determined using a NanoDrop One device (ThermoFisher).

cDNA synthesis and primer screening

Viral RNA was converted to cDNA using the High-Capacity cDNA Reverse Transcription Kit (Thermofisher), following the manufacturer's instructions. 10 µl of extracted RNA was input into a 20 µL cDNA synthesis reaction. For the primer screen, 1 µL of viral cDNA was used as input for primer screens, limit of detection test, and cross-reactivity screen RPA reactions. 1 µl of water was used as input for negative controls.

RT-RPA reactions using unlabeled primers

RPA reactions were conducted using the TwistAmp Basic Lyophilized kit (TwistDx), following the manufacturer's instructions, but were scaled down from a 50 µL reaction to a 10 µL reaction. In brief, the lyophilized mix was rehydrated using 29.5 µL of the provided rehydration buffer and 10 µL of nuclease-free water. 7.9 µL of the rehydrated mix was used per 10 µL reaction, along with 0.3 µM of each primer, 280 mM magnesium acetate, and 1µL of cDNA. The reactions were incubated for 20 minutes at either 37°C, 39°C, or 42°C. Diluted reaction products (2:1) were run on a 2.5% agarose gel (BioRad) in 1x TAE buffer (BioRad) for 30 minutes at 100 volts.

RT-RPA reactions using labelled primers

For the hybridization method, reactions were set up as described as above, with one minor change, where the reverse primer was replaced with a reverse primer with a 5'biotin labelled version, with the same primer concentration in the reaction. The hybridization step was performed as described by Qian's hybridization protocol [43], using a probe that was labeled with a 5'-FAM tag (Supplementary Table 1). Following the RPA reaction run, 1 µL of 5 µM hybridization probe (final concentration of 0.167 µM) and 19 µL of hybridization buffer (10 mM Tris HCl at pH 8.5) were added to each reaction. This reaction mix was heated to 95°C for 3 minutes on the thermocycler and then cooled to room temperature to allow for the hybridization reaction.

Detection of RPA products on LFA strips

The products from the hybridization and reactions were processed using the HybriDetect 2T LFA strips (Milenia Biosciences), following the manufacturer's instructions. Unpurified reaction products were diluted in the provided assay buffer (1:15

for hybridization reactions) and applied to the strip. The strip was then immersed in 70 µL of the provided assay buffer and was allowed to react for 10-15 minutes. The strips were imaged using a smartphone camera.

qPCR

cDNA samples derived from mice brains were analyzed by qPCR using PowerTrack SYBR Green kit (ThermoFisher) to detect LACV. The following primers were used: forward (ATTCTACCCGCTGACCATTG) and reverse (GTGAGAGTGCCATAGCGTTG). qPCR was performed using a QuantStudio 3Flex instrument (Applied Biosystems). QuantStudio Real-Time PCR software was used to extract data. GAPDH was used as a control of expression for qPCR samples.

Infection of mice with LACV and timepoint collection

All animal studies were approved by the Rutgers University IACUC (protocol number 202300007) and performed in accordance with protocols set forth by the National Institutes of Health *Guide for the Care and Use of Laboratory Animals* and ARRIVE guidelines. Wildtype (C57BL/6) mice were purchased from Jackson Laboratories and maintained in a breeding colony at the Child Health Institute of New Jersey. Weanling (3 weeks old) and adult mice (8 weeks old) were inoculated with 10^3 PFU of LACV in phosphate-buffered saline (PBS) intraperitoneally in a volume of 100 µl/mouse. Mice were observed daily for signs of neurological disease that included abnormal gait, seizures, and lethargy beyond collection timepoint. Animals with clinical

signs of neurological disease were scored as clinical and euthanized immediately and humanely and either used or not used in the studies listed above based on death date. Mice brains were then collected at the following timepoints: 2, 3, 4, 5, and 7 days post-infection for weanlings and 4, 5, 6 ,7, 10 and 20 days post-infection for adults and were stored in RNAse away, as previously described [20, 22]. Viral RNA was extracted as described.

Acknowledgements

We would like to thank Rutgers Global Health Institute, Rutgers Robert Wood Johnson Medical School, and The Child Health Institute of New Jersey for their continued support.

Author Contributions

LL designed probes and primers, planned, ran most of the experiments described above, analyzed experimental data, and wrote the original draft of manuscript. LL and BBH planned and carried out experiments. RA assisted with mouse infections, mouse monitoring, and brain collection. SS helped with the development of probes, primers and protocol optimization. BBH developed the ideas for the paper, as well as supervised the work, and planned and carried out experiments. All authors contributed to the interpretation of the data and played a role in reviewing and editing the manuscript.

Data Availability Statement

Data produced as part of the current study are available in the manuscript or upon request from the corresponding author.

Competing Interests Statement

BBH is a co-founder of Mir Biosciences, Inc., a biotechnology company focused on T cell-based diagnostics and vaccines for infectious diseases, cancer, and autoimmunity.

References

1. Alatrash, R. and B.B. Herrera, *The Adaptive Immune Response against Bunyavirales.* Viruses, 2024. **16**(3).
2. Evans, A.B. and K.E. Peterson, *Throw out the Map: Neuropathogenesis of the Globally Expanding California Serogroup of Orthobunyaviruses.* Viruses, 2019. **11**(9).
3. Soldan, S.S., et al., *La Crosse virus nonstructural protein NSs counteracts the effects of short interfering RNA.* J Virol, 2005. **79**(1): p. 234-44.
4. Blakqori, G., et al., *La Crosse bunyavirus nonstructural protein NSs serves to suppress the type I interferon system of mammalian hosts.* J Virol, 2007. **81**(10): p. 4991-9.
5. Soldan, S.S., et al., *La Crosse virus (LACV) Gc fusion peptide mutants have impaired growth and fusion phenotypes, but remain neurotoxic.* Virology, 2010. **404**(2): p. 139-47.
6. Reese, S.M., et al., *Potential for La Crosse virus segment reassortment in nature.* Virol J, 2008. **5**: p. 164.
7. Bennett, R.S., et al., *Genome sequence analysis of La Crosse virus and in vitro and in vivo phenotypes.* Virol J, 2007. **4**: p. 41.
8. Arragain, B., et al., *Structural snapshots of La Crosse virus polymerase reveal the mechanisms underlying Peribunyaviridae replication and transcription.* Nat Commun, 2022. **13**(1): p. 902.

9. Day, C.A., A. Odoi, and R. Trout Fryxell, *Geographically persistent clusters of La Crosse virus disease in the Appalachian region of the United States from 2003 to 2021.* PLoS Negl Trop Dis, 2023. **17**(1): p. e0011065.
10. McJunkin, J.E., R.R. Khan, and T.F. Tsai, *California-La Crosse encephalitis.* Infect Dis Clin North Am, 1998. **12**(1): p. 83-93.
11. Goldman, T. and D.H. Hamer, *Current Status of La Crosse Virus in North America and Potential for Future Spread.* Am J Trop Med Hyg, 2024. **110**(5): p. 850-855.
12. Haddow, A.D. and A. Odoi, *The incidence risk, clustering, and clinical presentation of La Crosse virus infections in the eastern United States, 2003-2007.* PLoS One, 2009. **4**(7): p. e6145.
13. Prevention, U.S.C.f.D.C.a. *La Cross Virus*. 2024 5/15/2024 [cited 2025 1/3/2025].
14. Gaensbauer, J.T., et al., *Neuroinvasive arboviral disease in the United States: 2003 to 2012.* Pediatrics, 2014. **134**(3): p. e642-50.
15. Evans, A.B., C.W. Winkler, and K.E. Peterson, *Differences in Neuropathogenesis of Encephalitic California Serogroup Viruses.* Emerg Infect Dis, 2019. **25**(4): p. 728-738.
16. Lau, L., et al., *Snowshoe Hare Virus Causing Meningoencephalitis in a Young Adult From Northern Manitoba, Canada.* Open Forum Infect Dis, 2017. **4**(3): p. ofx150.
17. Boutzoukas, A.E., et al., *La Crosse Virus Neuroinvasive Disease in Children: A Contemporary Analysis of Clinical/Neurobehavioral Outcomes and Predictors of Disease Severity.* Clin Infect Dis, 2023. **76**(3): p. e1114-e1122.
18. Harding, S., et al., *La Crosse virus: a scoping review of the global evidence.* Epidemiol Infect, 2018. **147**: p. e66.
19. Day, C.A., B.D. Byrd, and R.T. Trout Fryxell, *La Crosse virus neuroinvasive disease: the kids are not alright.* J Med Entomol, 2023. **60**(6): p. 1165-1182.
20. Basu, R., et al., *Identification of age-specific gene regulators of La Crosse virus neuroinvasion and pathogenesis.* Nat Commun, 2023. **14**(1): p. 2836.
21. Alatrash, R., V. Vaidya, and B.B. Herrera, *Age-specific dynamics of neutralizing antibodies, cytokines, and chemokines in response to La Crosse virus infection in mice.* J Virol, 2024. **98**(12): p. e0176224.
22. Basu, R., et al., *Age influences susceptibility of brain capillary endothelial cells to La Crosse virus infection and cell death.* J Neuroinflammation, 2021. **18**(1): p. 125.
23. Teleron, A.L., et al., *La Crosse Encephalitis: An Adult Case Series.* Am J Med, 2016. **129**(8): p. 881-4.
24. Wasieloski, L.P., Jr., et al., *Reverse transcription-PCR detection of LaCrosse virus in mosquitoes and comparison with enzyme immunoassay and virus isolation.* J Clin Microbiol, 1994. **32**(9): p. 2076-80.
25. Watzinger, F., K. Ebner, and T. Lion, *Detection and monitoring of virus infections by real-time PCR.* Mol Aspects Med, 2006. **27**(2-3): p. 254-98.
26. Lambert, A.J., et al., *Nucleic acid amplification assays for detection of La Crosse virus RNA.* J Clin Microbiol, 2005. **43**(4): p. 1885-9.
27. Salcedo, N., et al., *Comparative Evaluation of Rapid Isothermal Amplification and Antigen Assays for Screening Testing of SARS-CoV-2.* Viruses, 2022. **14**(3).

28. Evans, A.B. and K.E. Peterson, *Cross reactivity of neutralizing antibodies to the encephalitic California Serogroup orthobunyaviruses varies by virus and genetic relatedness.* Sci Rep, 2021. **11**(1): p. 16424.
29. Daher, R.K., et al., *Recombinase Polymerase Amplification for Diagnostic Applications.* Clin Chem, 2016. **62**(7): p. 947-58.
30. Faye, M., et al., *A recombinase polymerase amplification assay for rapid detection of rabies virus.* Sci Rep, 2021. **11**(1): p. 3131.
31. Vasileva Wand, N.I., et al., *Point-of-care diagnostic assay for the detection of Zika virus using the recombinase polymerase amplification method.* J Gen Virol, 2018. **99**(8): p. 1012-1026.
32. Lobato, I.M. and C.K. O'Sullivan, *Recombinase polymerase amplification: Basics, applications and recent advances.* Trends Analyt Chem, 2018. **98**: p. 19-35.
33. Sainetra Sridhar, P.B.T., Lily Lumkong, Eduardo Martins Netto, Carlos Brites, Wei-Kung Wang & Bobby Brooke Herrera, *RT-RPA as a dual tool for detection and phylogenetic analysis of epidemic arthritogenic alphaviruses.* Scientific Reports, 2024. **14**.
34. Jauset-Rubio, M., et al., *Ultrasensitive, rapid and inexpensive detection of DNA using paper based lateral flow assay.* Sci Rep, 2016. **6**: p. 37732.
35. Shelite, T.R., et al., *Isothermal recombinase polymerase amplification-lateral flow detection of SARS-CoV-2, the etiological agent of COVID-19.* J Virol Methods, 2021. **296**: p. 114227.
36. Ghosh, D.K., S.B. Kokane, and S. Gowda, *Development of a reverse transcription recombinase polymerase based isothermal amplification coupled with lateral flow immunochromatographic assay (CTV-RT-RPA-LFICA) for rapid detection of Citrus tristeza virus.* Sci Rep, 2020. **10**(1): p. 20593.
37. Davis, J., et al., *Endemic La Crosse Virus Neuroinvasive Disease in North Carolina Residents: 2000-2020.* N C Med J, 2024. **85**(4): p. 289-295.
38. Taylor, K.G., et al., *Age-dependent myeloid dendritic cell responses mediate resistance to la crosse virus-induced neurological disease.* J Virol, 2014. **88**(19): p. 11070-9.
39. Bennett, R.S., et al., *La Crosse virus infectivity, pathogenesis, and immunogenicity in mice and monkeys.* Virol J, 2008. **5**: p. 25.
40. Evans, A.B., C.W. Winkler, and K.E. Peterson, *Differences in neuroinvasion and protective innate immune pathways between encephalitic California Serogroup orthobunyaviruses.* PLoS Pathog, 2022. **18**(3): p. e1010384.
41. Calisher, C.H., et al., *Serodiagnosis of La Crosse virus infections in humans by detection of immunoglobulin M class antibodies.* J Clin Microbiol, 1986. **23**(4): p. 667-71.
42. Pierson, T.C. and M.S. Diamond, *The continued threat of emerging flaviviruses.* Nat Microbiol, 2020. **5**(6): p. 796-812.
43. Qian, J., et al., *An enhanced isothermal amplification assay for viral detection.* Nat Commun, 2020. **11**(1): p. 5920.

Tables

Table 1. Nucleic acid sequence homology of the S, M, and L segments between LACV and other related bunyaviruses

Virus	S Segment Homology	M Segment Homology	L Segment Homology
La Crosse virus	100%	100%	100%
Snowshoe hare virus	88%	78.8%	81.6%
Khatanga virus	87%	77.5%	78%
California encephalitis virus	79.8%	73.6%	76.9%
Tahyna virus	82.2%	73%	77.3%
Lumbo virus	80.7%	72.3%	76.7%
San Angelo virus	80.1%	70.5%	77.1%
Jamestown Canyon virus	76.1%	69%	73.7%

Figures

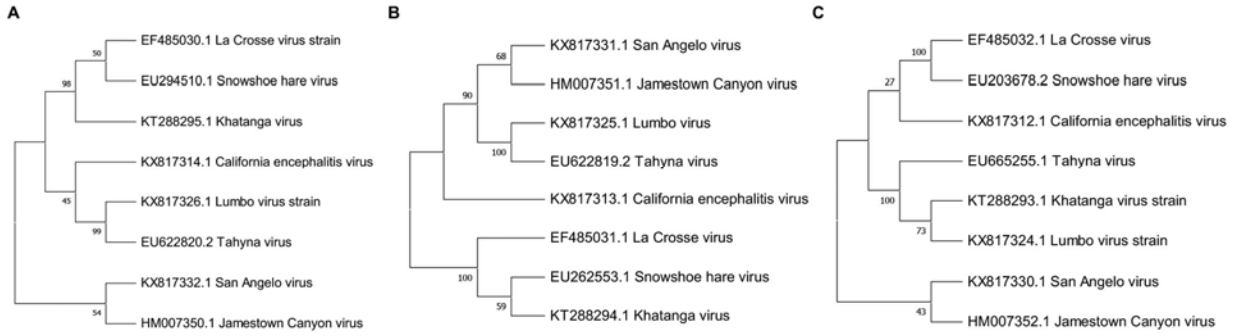

Fig. 1 Phylogenetic trees of the S, M, L segments of LACV and related bunyaviruses. Phylogenetic trees were constructed from aligning nucleotide sequences of the A) small (S), B) medium (M), and C) large (L) segments from bunyaviruses within the CSG, including La Crosse virus, Snowshoe hare virus, Khatanga virus, California Encephalitis virus, San Angelo virus, Lumbo virus, and Tahnya virus, and Melaka virus (MELV) family, including Jamestown Canyon virus. The sequences were aligned using Clustal omega, and the resulting alignments were used to construct maximum-likelihood trees based on the Tamura-Nei model and 500 bootstrapping replications using Mega11. Associated accession numbers are included by the name of each virus for each tree.

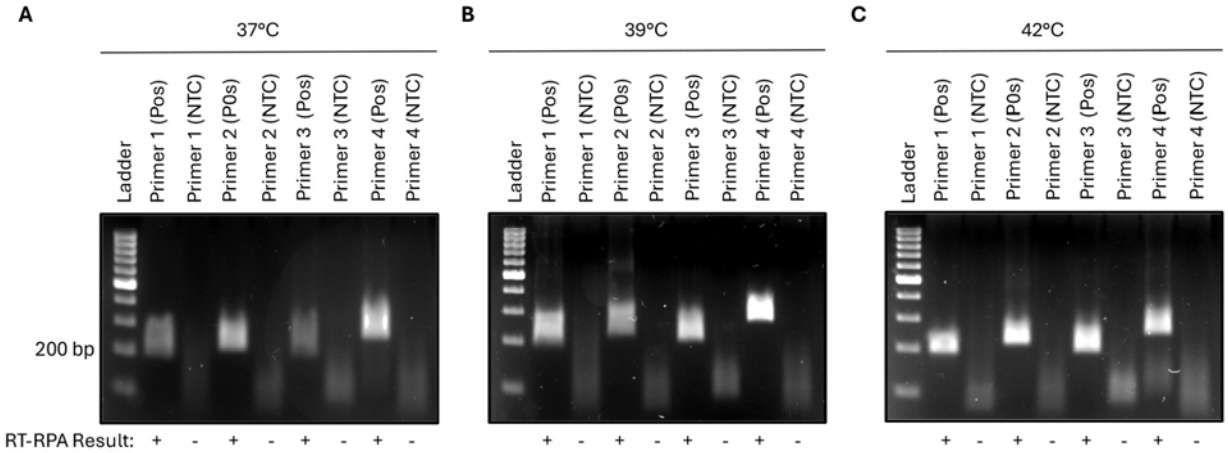

Fig. 2 Primer screen RT-RPA testing. Primer screen RT-RPA testing at A) 37°C, B) 39°C, and C) 42°C using 4 different primer pairs. Primer pair 3 at 39°C was chosen for further experimentation. Pos, positive control, La crosse virus cDNA input. NTC, no template control, water input. +, positive result. -, negative result.

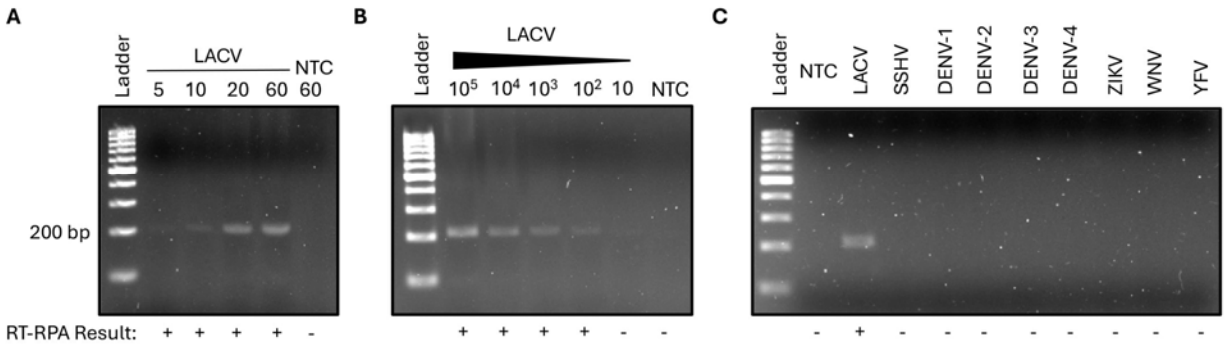

Fig. 3 Time Course, limit of detection, and cross-reactivity RT-RPA testing with visualization of results via gel electrophoresis. A) Time course tests were performed at 5 minutes, 10 minutes, 20 minutes and 60 minutes. The time course was optimized at 20 minutes. B) Viral RNA from 10^5 copies to 0 copies was reverse transcribed to cDNA and used in RT-RPA testing. The limit of detection was determined to be between 100 to 1000 viral copies. C) RT-RPA was performed using cDNA from La Crosse virus (LACV), Snowshoe hare virus (SSHV), dengue virus serotype 1 (DENV-1), dengue virus serotypes 2 (DENV-2), dengue virus serotype 3 (DENV-3), dengue virus serotype 4 (DENV-4), Zika virus (ZIKV), West Nile virus (WNV), or yellow fever virus (YFV). No cross-reactivity was observed.

NTC, no template control, water input. +, positive result. -, negative result.

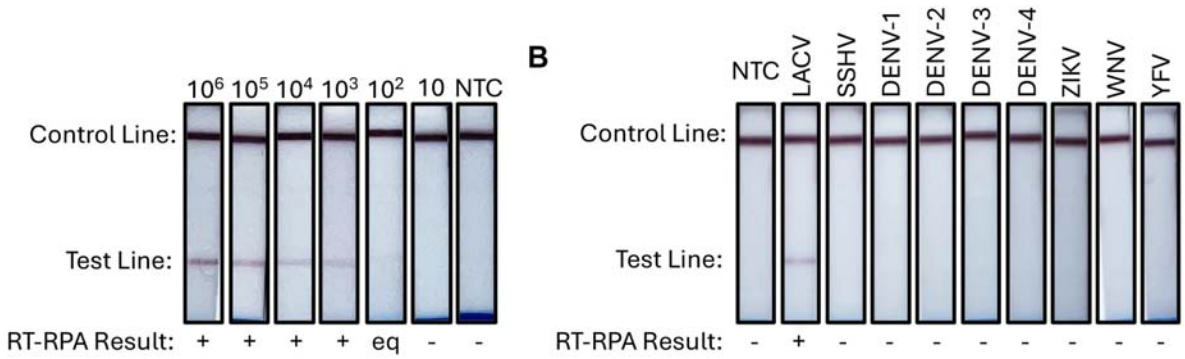

Fig. 4. RT-RPA limit of detection and cross-reactivity testing with visualization of results via LFA strips. A) Viral RNA from 10^5 copies to 0 copies was reverse transcribed to cDNA and used in RT-RPA testing. The limit of detection was determined to be between 100 to 1000 viral copies. Results that were equivocal were indicated by "eq". B) RT-RPA was performed using cDNA from La Crosse virus (LACV), Snowshoe hare virus (SSHV), dengue virus serotype 1 (DENV-1), dengue virus serotypes 2 (DENV-2), dengue virus serotype 3 (DENV-3), dengue virus serotype 4 (DENV-4), Zika virus (ZIKV), West Nile virus (WNV), or yellow fever virus (YFV). No cross-reactivity was observed. NTC, no template control, water input. +, positive result. -, negative result. eq, equivocal result.

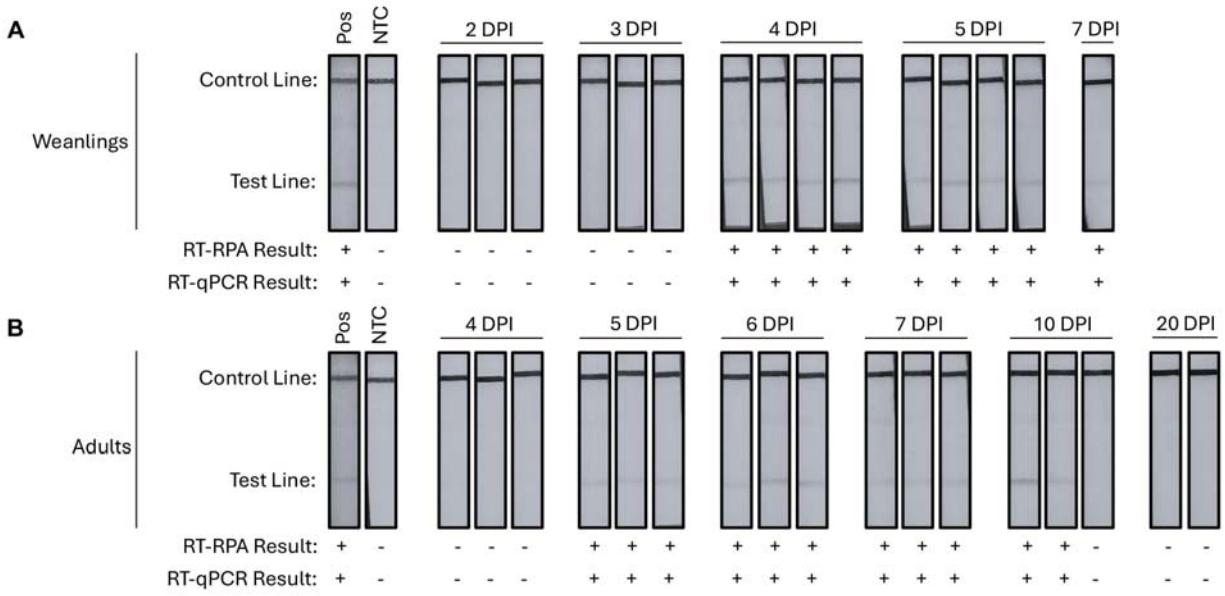

Fig. 5. LACV neuroinvasion into the brain of weanling and adult mice visualized by LFA strips. Mice were infected with 1000 plaque forming units of LACV and mice were humanely sacrificed and brains were collected 2-7 days post-infection (DPI) for weanlings and 4-20 dpi for adults. A) LACV was detected in the brain in weanling mice by both RT-RPA and RT-qPCR as early as 4 DPI. B) LACV was detected in the brain in adult mice by both RT-RPA and RT-qPCR by 5 DPI with clearance of the virus by 20 DPI. Pos, positive control, La crosse virus cDNA input. NTC, no template control, water input. +, positive result. -, negative result.

Supplementary Figure

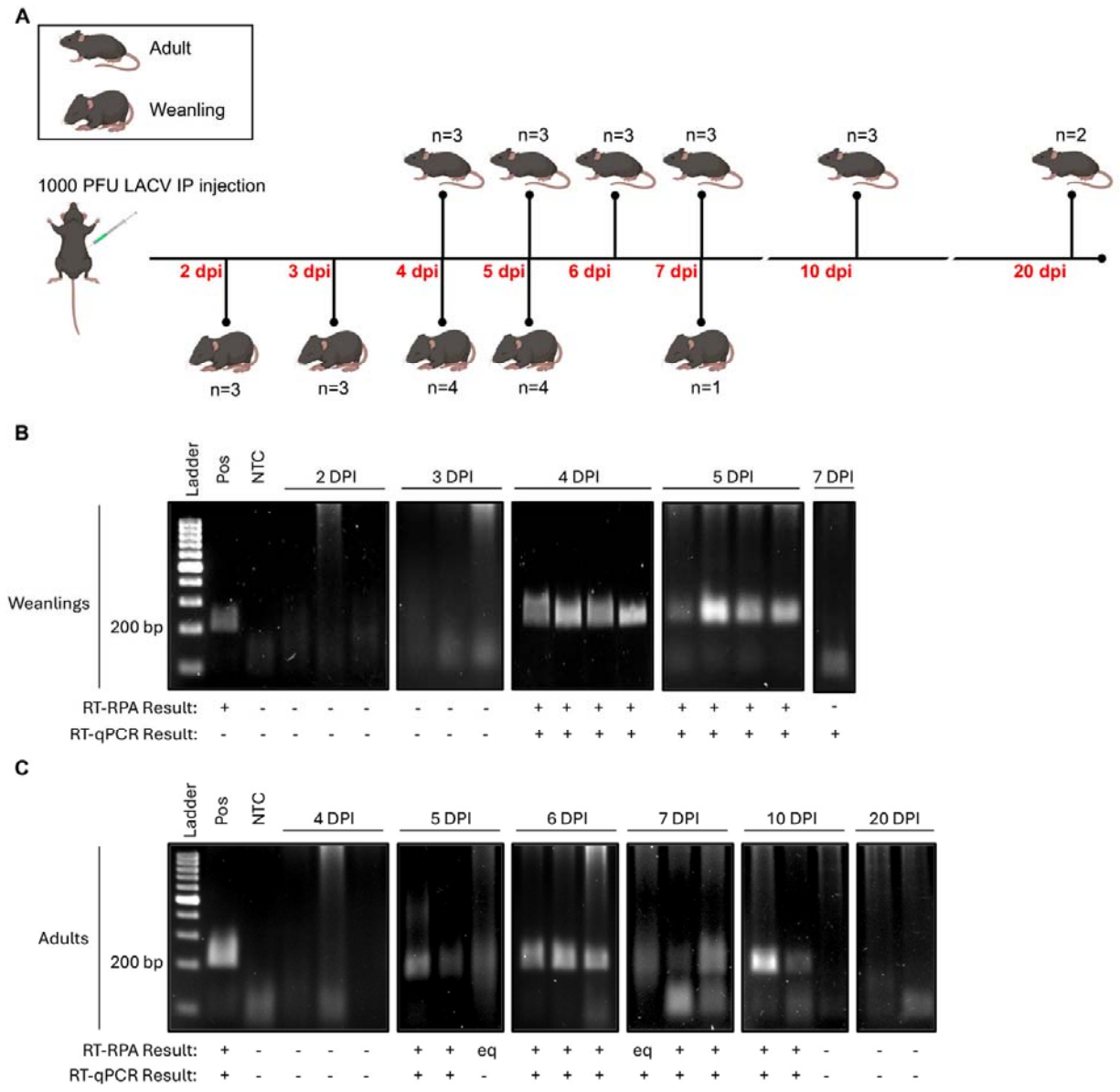

Supplementary Fig. 1. Serial euthanasia schematic and LACV neuroinvasion into the brain of weanling and adult mice visualized by gel electrophoresis. A) Mice were infected with 1000 plaque forming units of LACV and mice were humanely sacrificed, and brains were collected 2-7 days post-infection (DPI) for weanlings and 4-20 dpi for adults. B) LACV was detected in the brain in weanling mice by both RT-RPA and RT-qPCR as early as 4 DPI. C) LACV was detected in the brain in adult mice by

both RT-RPA and RT-qPCR by 5 DPI with clearance of the virus by 20 DPI. DPI, days post-infection. Pos, positive control, La crosse virus cDNA input. NTC, no template control, water input. +, positive result. -, negative result. eq, equivocal result.

Supplementary Table

Supplementary Table 1. RT-RPA primer pairs and hybridization probe.

Primer Pair	Forward	Reverse	Amplicon Size
1	GTCTTGTTATCATTGGATTGTTGATCGGGCTGC	CCTGTGAGCCATCAAACCTGCAGCATCTTC	204
2	CAACCCAGCAAAGGCCTCAAACCTTGCTAGAGG	TGATCAGTGCTAGATTGGAATACACCACCTGATGG	228
3 (unlabeled)	**TGATTACCAAGCATGCAAATTCCTTCAAAGCCC**	**TTCGAAGCAGTTAATACAGCCGGTGCATGACCC**	**208**
3 (labeled reverse)	**TGATTACCAAGCATGCAAATTCCTTCAAAGCCC**	**/5Biosg/TTCGAAGCAGTTAATACAGCCGGTGCATGACCC**	**208**
4	CCTGACGTAAAGCTCATCCAAGAAGGCGATGGG	CGCTATGCTAGATCTGCTTACTTGCCAATTACAG	240
Hybridization Probe	**/56-FAM/GTGGCACTGTGACCATAA**		

572